

EPA

Feasibility Study to Evaluate a Gold External Standard for Use in XRF Screening of Lead

Phase II



FEASIBILITY STUDY TO EVALUATE A GOLD EXTERNAL STANDARD FOR
USE IN XRF SCREENING OF LEAD IN PAINT
PHASE II

by □

Jan Eric Kilduff
Lockheed Martin Sciences Group
980 Kelly Johnson Dr.
Las Vegas, Nevada 89119

Contract 68-C5-0091

Technical Monitor

Brian A. Schumacher

Characterization Research Division
National Exposure Research Laboratory
P.O. Box 93478, Las Vegas, NV 89193-3478

NATIONAL EXPOSURE RESEARCH LABORATORY
OFFICE OF RESEARCH AND DEVELOPMENT
U. S. ENVIRONMENTAL PROTECTION AGENCY
LAS VEGAS, NV 89119

Notice

The U.S. Environmental Protection Agency (EPA), through its Office of Research and Development (ORD), partially funded and managed the research described here. It is intended for EPA internal use only. Mention of trade names or commercial products does not constitute endorsement or recommendation for use.

Table of Contents

Notice	ii
Tables	v
Figures	v
Executive Summary	vi
1. Introduction	1
2. Goals	1
3. Background	1
4. Phase II: Feasibility Study Approach	2
4.1. X-ray Spectral Characteristics	2
4.2. Detector Sensitivity	3
4.3. Model Experimental Observations	3
5. Equipment and Materials	4
5.1. Instrumentation	4
5.2. Materials	4
5.2.1. Metal Foils and Plastic Film	4
5.2.2. NIST Paint SRMs	4
6. Procedure	5
6.1. Field XRF	5
6.1.1. Detector Sensitivity	5
6.1.2. Gold External Standard	5
6.1.3. Titanium Film Coverlayer	6
6.2. Laboratory XRF	6
6.2.1. Gold External Standard	6
6.2.2. Titanium Foil and Plastic Film Coverlayers	6
7. Results and Discussion	7
7.1. Field XRF	7
7.1.1. Spectral Characteristics	7
7.1.2. Detector Response	7
7.1.3. Gold External Standard	8
7.1.4. Titanium Foil Coverlayers	10
7.2. Laboratory XRF	10
7.2.1. Metal Foil and Plastic Film Coverlayers	12
7.2.2. Application of the Gold External Standard	13
8. Summary	16

9. References 17

Appendix A-1

Definitions A-1

Tables

Table 1.	Measured and calculated XRF variables evaluated for identifiable relationships.	3
Table 2.	NIST lead-based paint SRMs	5
Table 3.	The HNu Si(Li) detector response to Pb K- and L-line X-rays.	8
Table 4.	Data showing the gold external standard effects on lead calibration data.	9
Table 5.	Lead calibration and replicate analysis data in the presence of titanium coverlayers	10
Table 6.	Lead calibration data in the presence of metal and plastic cover materials, using the ratio of the silver Compton and lead $L\beta$ counts to extend the linear range of the calibration. . . .	12
Table 7.	Rate changes of gold $L\beta/L\alpha$ line ratio versus coverlayer thickness.	15

Figures

Figure 1.	XRF spectrum of 1.02 mg/cm ² NIST paint on wallboard.	7
Figure 2.	XRF spectrum of 1.02 mg/cm ² NIST paint with gold disk on wallboard.	9
Figure 4.	Laboratory XRF spectrum of 1.02 mg/cm ² NIST lead-based paint with gold external standard, demonstrating complete resolution of lead and gold X-rays.	11
Figure 5.	Saturation of XRF lead $L\beta$ X-rays are observed at high lead concentrations.	11
Figure 6.	Lead calibration curve with lead $L\beta/Ag$ Compton ratio versus concentration.	11
Figure 7.	Titanium coverlayers reduce sensitivity of XRF to changes in lead concentration.	13
Figure 8.	Relative peak height differences of gold and lead L-line X-rays with increasing thickness of titanium coverlayers over lead-based paint using silver X-rays for excitation.	14
Figure 9.	Effect of titanium coverlayers on gold $L\beta/L\alpha$ X-ray line ratios.	15
Figure 10.	Effect of titanium coverlayers on lead $L\beta/L\alpha$ X-ray line ratios.	15

Executive Summary

Lead-based paint coating the interior of urban dwellings and paint remnants residing in soil are recognized as potential sources for lead exposure in urban areas. Portable X-ray fluorescence (XRF) instruments are commonly employed to screen facilities suspected of containing materials that exceed regulatory limits for lead in painted wall surfaces. These instruments provide rapid results with nondestructive testing. Current XRF measurement techniques are subject to substrate and matrix effects which can result in an over- or under-estimation of the lead concentration. The EPA's Characterization Research Division in Las Vegas (CRD-LV) has begun a three-phase feasibility study to determine if analytical protocols for lead determinations by XRF can be developed that use an insertable gold-based external standard material to eliminate false negatives in lead detection and increase the accuracy of the quantitative results. Phase I focused on preparation of reference materials and training of staff. Phase II, described in this report, evaluated the spectral characteristics of lead X-rays from lead-based paint and gold X-rays from the standard material. Phase III will involve development of an X-ray intensity correction protocol and development of recommendations for its use in routine lead determinations.

For Phase II, false negative conditions for K- and L-line X-rays of lead and gold were simulated using titanium, aluminum, and acetate-film cover materials. The feasibility of a gold external standard used in conjunction with a field XRF instrument equipped with a high-resolution Si(Li) detector was demonstrated for K- and L-line X-rays. The high-energy K-line X-rays from the gold were unaffected by the cover materials and served only to indicate X-ray penetration to the substrate. The lead and gold L-line X-rays were sufficiently broadened so that overlap occurred, which was a result of the instrument geometry and the high-energy X-rays emitted by the Co⁵⁷ source. An alternative external standard material, such as platinum, which is uncommon in the environment and free from interference in the field XRF, is suggested as a more feasible choice.

The gold external standard was also feasible for making L-line determinations of lead using a laboratory XRF instrument. The maximum linear range for lead calibrations was achieved using the ratio of the lead

$L\alpha$ and the silver Compton scatter X-rays versus lead concentration. The titanium, aluminum, and plastic cover materials were shown experimentally to be sources that result in false negatives for the XRF determination of lead. A gold external standard, placed beneath the paint standard reference material, was free of interferences from materials in the paint matrix and had no effect on the lead calibration curve. The value for the ratio of the gold $L\alpha/L\beta$ X-rays increased as the thickness of a cover material was increased. This change in the gold $L\alpha/L\beta$ ratio is relatively independent of lead concentration, changing only with increasing cover material thickness. The slope or rate of change of gold $L\alpha/L\beta$ ratio versus cover material thickness was proportional to the magnitude of the mass absorption coefficients of the cover material.

The feasibility of using a gold external standard to eliminate one source of false negatives in the XRF determination of lead has been demonstrated in this Phase II work. Additional work is necessary to develop a general expression to calculate intensity corrections for the lead L-lines when coverlayers are present, account for changes in the coverlayer mass absorption coefficients, and investigate other external standard materials that would be useful in both K- and L-line XRF instruments. This work will be completed in Phase III.

1. Introduction

Federal, state, and local governments have begun expanding programs for the sampling and determination of lead due to continuing reports of its adverse health effects, especially on children¹. Lead-based paint that coats the interior of urban dwellings and paint remnants that reside in soil are recognized as sources for lead exposure in urban areas. The Lead-Based Paint Poisoning Prevention Act, 42, U.S.C., 1971, requires that public housing authorities implement programs to randomly inspect all housing projects for lead-based paint by 1994. Facilities found to exceed the regulatory limit of 1.0 mg/cm² for lead in painted wall surfaces are required to implement procedures to reduce (or abate) the lead levels below the mandated level.

The sheer number of facilities requiring inspection has resulted in the use of portable X-ray fluorescence (XRF) instruments as a preferred screening method. Portable XRF instruments provide rapid results with nondestructive testing. Current XRF measurement techniques, however, are subject to substrate and matrix effects that can result in over- or under-estimation of the lead concentration^{2,3}. Consequently, all field measurements are subject to laboratory confirmation to verify the lead concentration, creating an additional burden on project sampling and analysis plans and costs. The possibility for false negatives for lead is particularly troublesome because of the associated unknown exposure levels from an environment that is supposed to be “clean.”

2. Goals

The EPA's Characterization Research Division in Las Vegas (CRD-LV) has begun a feasibility study concerning the elimination of possible false negatives associated with the XRF detection and quantitation of lead in painted surfaces and associated with soils contaminated with lead originating from lead-based paints. A secondary goal is to determine the factors that affect the intensity of the lead X-rays to allow intensity corrections to be made. This knowledge is especially important in conducting XRF analyses utilizing the low-energy L-line X-rays, which can be attenuated by paint coverlayers thereby resulting in negative bias for lead quantitation⁴. Lockheed Environmental Systems & Technologies Company (LESAT) has been tasked to evaluate significant variables involved in the XRF determination of lead in painted surfaces and soils. The study is intended to determine if analytical protocols for lead determinations by XRF can be developed that use an insertable external standard to eliminate false negatives and increase the accuracy of the quantitative results.

3. Background

Portable X-ray fluorescence analyzers exhibit some difficulties in the measurements of lead in painted surfaces, such as walls, doors, and window casements, as well as in soils. The possibility of using an external standard to solve some of these difficulties was considered during a technical discussion between L. R. Williams and H. A. Vincent, both with EPA, CRD-LV⁵.

The minimum requirements for the externally applied standard were as follows:

- The X-ray lines from the external standard must be close in energy to the X-ray lines for lead.
- The external standard X-ray lines must be resolvable from the X-ray lines of lead.
- The energy of the external standard X-rays must not exceed the absorption edge for lead X-rays.

A material ideally suited to serve as an external standard is a thin layer of gold coated on an insertable probe. By controlling the depth to which the gold-coated probe is inserted into the soil or paint matrix, gold X-ray line intensity data can be used to ascertain the magnitude of the corresponding matrix or substrate absorbance effects on the lead X-ray line intensities. In the simplest case, the absence or significant reduction of the gold X-ray line intensities would indicate potential interference to the lead X-ray lines. In the ideal case, changes in gold X-ray line intensities may be used as potential calibration/correction factors to adjust lead X-ray line intensities to be proportional to true lead concentration.

A study evaluating the use of gold as an external standard is being conducted in three phases. Phase I experimental work, completed in FY 1993⁶, began with the preparation of reference pellets from nine well-characterized urban soils. Changes in the XRF spectra of the pellets in the presence of a gold foil on the side opposite the X-ray beam exit were examined. Staff were also trained and licensed to use an HNu SEFA PbTM XRF instrument for work to be performed during FY 1994. In FY 1994, Phase II was completed and is described in this report. Phase III, to be completed in FY 1995, will involve development of an X-ray intensity correction protocol for L-line X-rays based upon empirical and/or theoretical models, calculation of detection limits for L-line X-rays, determination of optimum configuration for an external standard for use with L-line X-rays, and an investigation on the feasibility of using metals other than gold as external XRF standards. Recommendations for incorporating this technology into working methods for lead determinations also will be developed in Phase III.

4. Phase II: Feasibility Study Approach

Spectral characteristics of the lead X-rays from lead-based paint, gold X-rays from the external standard material, and Compton* scatter in sample substrate but related to the excitation sources were evaluated under controlled conditions by using a laboratory XRF instrument and materials of known specification. The absorbance/enhancement effects of titanium (Ti), aluminum (Al), and acetate-film cover materials (i. e., covering the sample that contains lead) on the quantitation of lead using both K- and L-line X-rays were also examined. These materials are common in modern lead-free paints as pigments, extenders, or binders⁸. In paint, the elements Ti and Al are generally present as oxides. Pure-element metal foils (Ti and Al) of known thickness were appropriate simulations of the metal oxides because the chemical form or combination of an element is not critical in XRF measurements.

Experimental data for X-ray geometry, detector sensitivity, external standard, and film coverlayer effects were obtained by preparing appropriate calibration curves using National Institute of Standards and Technology (NIST) lead-based paint standard reference materials (SRMs). XRF measurements for the K- and L-line X-rays of lead were obtained for NIST paint films (1) with no external reference, (2) with the external reference located behind the paint film, and (3) with the external reference located behind the paint film and with metal foil or plastic film located in front of the paint film. The measurements were also used to study the effects of source energy differences and to prepare models of the experimental observations.

4.1. X-ray Spectral Characteristics

The X-ray spectra generated with the laboratory and portable XRF instruments were examined to determine if the external standard X-ray lines were well resolved from other component peaks present in the XRF spectrum. It was also desirable to have external X-rays in a region with a low background. This criterion was difficult to accomplish with the high-energy Co⁵⁷ source because its X-rays are capable of

exciting all elements present in a sample and cause enhancement to the lead or external reference X-rays, especially in the L-line region of the XRF spectrum.

X-ray spectra were then examined from the experiments with metal foil or plastic film coverlayers. Because the precise thickness of the overlying film was known, the mass absorption coefficients for the L-line X-rays could be calculated and compared to values given in the literature to ensure internal consistency of the data. Changes in L β /L α line intensity ratios from the gold external standard and the lead due to the addition of the shielding layers were studied for suitability to provide intensity correction information regarding the lead X-rays.

4.2. Detector Sensitivity

The field XRF instrument was used to measure lead and gold K α and K β X-ray line intensities to determine whether these high-energy X-rays display trends similar to those observed for the low-energy L-line X-rays. The K α and K β X-rays from lead and from the gold external standard were measured with the field and laboratory XRF instruments to evaluate the changes in line intensities due to the differences in source-sample-detector geometries and source energies of the two instruments.

4.3. Model Experimental Observations

The XRF calibration curve data were used to obtain quantitative data on the effects of different X-ray sources, instrument geometry, and overlying materials on X-ray intensities. A set of directly measured or calculated variables (Table 1) was examined to determine the feasibility for obtaining identifiable trends for these variables versus paint SRMs. X-ray line intensity data were collected with the paint SRMs, the gold external standard, and metal or plastic cover materials. The results were used to determine the minimum detectable surface area of gold external standard material located beneath a NIST paint layer and to establish corrections for overlying titanium or plastic layers.

Table 1. Measured and calculated XRF variables evaluated for identifiable relationships.

Element	Measured X-ray Lines	Calculated Variables
Gold	K α , K β	
Gold	L α , L β	Gold L β /gold L α
Lead	K α , K β	
Lead	L α , L β	Lead L β /lead L α
Silver	Compton Scatter	Gold L β /Ag Compton, lead L β /Ag Compton

5. Equipment and Materials

5.1. Instrumentation

The HNu field XRF consists of a probe which houses a high resolution Si(Li) detector (180 eV), a liquid nitrogen dewar and a Co⁵⁷ radioisotope. The Si(Li) detector is chilled by liquid nitrogen in the dewar. The annular radioisotope source contains three 3.3-mCi capsules (10 mCi total) held in a circle at 120° intervals with a tungsten holder. The tungsten holder containing the three Co⁵⁷ capsules encircles the Si(Li) detector resulting in a near 90° angle of incidence for the source X-rays and a 90° sample-to-detector take-off angle. Fluorescent X-ray photons are converted to pulses by the Si(Li) detector, are amplified, and are sent to a 1024 multi-channel analyzer (MCA) located in the battery pack. Raw XRF spectra were sent via an KS-232 serial port as raw ASCII format to a Microsoft Windows-based computer. Spectra were displayed and analyzed via a Microsoft Excel spreadsheet.

Most of the L-line studies were performed on the laboratory XRF, a Kevex Analyst 770, equipped with a side-window X-ray tube, a rhodium anode, a silver secondary target, and a 30-mm² Si(Li) liquid nitrogen cooled detector (180 eV). The Kevex source-to-detector geometry has a 45° angle of incidence from the silver secondary target to the sample and a 45° take-off angle from the sample to the Si(Li) detector. The Kevex electronics consist of a 4460 pulse processor, a 1024-channel MCA, and a 5230 analog-to-digital converter. The MCA has a nominal resolution of 40 eV/channel. The computer workstation is a PDP-1 1/44 microprocessor, a color monitor, and a dot-matrix printer. Raw XRF spectra were collected and processed using the Kevex XRF Toolbox software.

5.2. Materials

5.2.1. Metal Foils and Plastic Film

Gold foil, obtained from the Aldrich Chemical Company, was received as a 25-mm square with a thickness of 0.025 mm. The gold content was greater than 99.99%. When used in the circular 31-mm sample holder of the Kevex, approximately 83% coverage was achieved. For use with the HNu, the gold foil was punched into 7.94-mm (5/16 in.) and 3.18-mm (1/8 in) diameter disks with nominal areas of 49.48 and 7.912 mm², respectively.

Three thicknesses of titanium foils were used. Titanium foils, received as 50-mm squares, with thicknesses of 0.050 and 0.025 mm and purity greater than 99.98%, were obtained from Aldrich Chemical Company. Titanium foil, received as a 50-mm square, with a thickness of 0.006 mm and purity greater than 99.5%, was obtained from Johnson Matthey. Titanium sheets used on the Kevex were cut into 31-mm diameter disks, and those used on the HNu were used as received.

The plastic films used to simulate organic binders and emulsifiers in contemporary paints were represented with Hewlett Packard plastic acetate plotter film used for transparencies. Multiple films were stacked together above the selected paint SRM to achieve films of the desired thickness as listed in Table A2 in the Appendix to this report.

5.2.2. NET Paint SRMs

The lead-based paint SRM from the NIST⁹ is traceable to lead concentrations determined by isotope-dilution mass spectrometry. The SRM contains five mylar sheets 0.2 mm in thickness. There is a

0.04-mm layer of lead-based paint on four of the sheets. The lead was introduced chemically as lead chromate and lead molybdate. The fifth sheet consists of a lead-free lacquer layer and serves as a blank for matrix corrections. A clear plastic laminate covers the paint and lacquer layers to protect them from abrasion. The films are color coded for each lead concentration (Table 2). The SRMs used with the HNu were cut into 5.0 x 5.0-cm squares; those used with the Kevex were cut into 31-mm diameter disks and otherwise analyzed as received.

Table 2. NIST lead-based paint SRMs.

Paint Color ID	Lead Concentration (mg/cm²)
white	lead free
green	0.29
orange	1.02
dark yellow	1.63
yellow	3.53

6. Procedure

6.1. Field XRF

When required, the gold external standard or metal foil was attached to the paint SRM with cellophane tape. The paint SRM was centrally mounted at a premarked location on the XRF sample probe surface and taped along two edges. The HNu probe surface was then pressed flush to a slab of residential plasterboard (substrate) which was also mounted on cardboard to minimize any potential backscatter from the room wall. The HNu was activated for 5 minutes of live-time data collection. Raw spectral data were transferred by RS232 cable and commercial communications software to an IBM-compatible PC. The raw spectrum was imported into a Microsoft Excel spreadsheet configured to perform background subtraction. Previously defined regions of interest (ROIs) were integrated by summation of the net counts in each channel of the ROI. At this time, any changes or unusual spectral characteristics were noted. Observations and recommendations for further experiments were recorded in a laboratory notebook. This procedure was repeated for each of the five samples in the paint SRM until sufficient data were collected to generate a calibration curve.

6.1.1. Detector Sensitivity

The HNu was configured as described above. The paint SRM was used to obtain a calibration curve for lead. The baseline-corrected integrated areas for the lead K- and L-line X-rays were converted to counts per second (cps) and the lead L¹/K¹ and L²/K² line ratios were calculated.

6.1.2. Gold External Standard

The gold-foil standard was attached to the center of the backsurface of each paint SRM prior to data collection. Three lead calibration curves (6 total) were obtained: one with no gold present, a second with a 7.94-mm diameter (49.48 mm²) gold-film disk, and a third with a 3.18-mm diameter (7.92 mm²) gold film disk for the lead K¹ and K² X-ray lines. A linear regression analysis was performed to determine the effects of the gold on the slopes, y intercepts, and correlation coefficients for each test condition. The gold

area versus integrated counts per second was plotted. The minimum surface area was determined as three sigma above the background counts from gold in the Si(Li) detector.

6.1.3. Titanium Film Coverlayer

Titanium squares, 50-mm per side and 0.050, 0.025, and 0.006 mm in thickness, were mounted on the front side of a paint SRM of the same size. A lead calibration curve was generated using each foil thickness with each of the five samples in the paint SF&I. A total of 21 measurements were made. For each thickness of titanium and each SRM sample (except for the 1.02-mg/cm² sample), one XRF measurement was made. On the 1.02-mg/cm² sample, three replicate measurements were made to more precisely determine the shielding effects, if any, from the titanium.

6.2. Laboratory XRF

Prior to quantitation, the X-ray spectra collected on the Kevex were processed to remove escape peaks; the background was auto-subtracted; and the analytical peaks of interest were deconvoluted using a Gaussian mathematical treatment.

The operating conditions used for the Kevex for analysis were:

- Secondary Target - Silver
- X-ray tube voltage - 35 KeV
- X-ray tube current - 3.0 mA
- time constant - 4.5 msec
- counting time - 200 set live time

6.2.1. Gold External Standard

The gold external standard consisted of a 25-mm square of gold foil that was attached behind each 31-mm diameter paint disk. Lead calibration curves were obtained. The gold foil was placed on the back side of each paint SRM to maximize the gold X-ray counts, thereby making trends of intensity changes more apparent.

Only the 25-mm-square gold external standard was studied in this phase of the project. Experiments to determine the minimum detectable area of external standard for an L-line XRF determination of lead will be performed in Phase III.

6.2.2. Titanium Foil and Plastic Film Coverlayers

Titanium circles, 31 mm in diameter and 0.050, 0.025, and 0.006 mm in thickness, were mounted on the front side of each paint SRM sample of the same size. A lead calibration curve was generated for each foil thickness with each of the five paint samples in the paint SRM. The 25-mm-square gold foil was behind the paint for all but one series of tests (Appendix, Table 2, spectra 26 through 30).

Plastic film circles, 31 mm in diameter and 0.830, 0.593, and 0.356 mm in thickness, were mounted on the front side of each paint SRM sample of the same size. Procedures identical to those used for the titanium foils were then followed.

7. Results and Discussion

7.1. Field XRF

7.1.1. Spectral Characteristics

The HNu field XRF instrument was used to simulate a typical K-line instrument with the resolution of a Si(Li) detector. A 5-minute live-time data collection interval typically required 9 minutes of elapsed time. Long data-collection times were used to minimize background noise and to allow more accurate integration of the peaks. Typically, when the HNu is used in field sampling to acquire large numbers of samples, the sampling interval is 10 to 30 seconds.

The XRF spectrum of the 1.02-mg/cm² paint SRM shows lead K- and L-line X-rays (Figure 1, points E and A). The K-lines are free of interferences whereas the L-lines are not. The Si(Li) detector is more sensitive to the L-lines for the equivalent concentration of lead. The high-energy lead K-line X-rays might be better detected with a germanium-lithium Ge(Li) detector.¹⁰

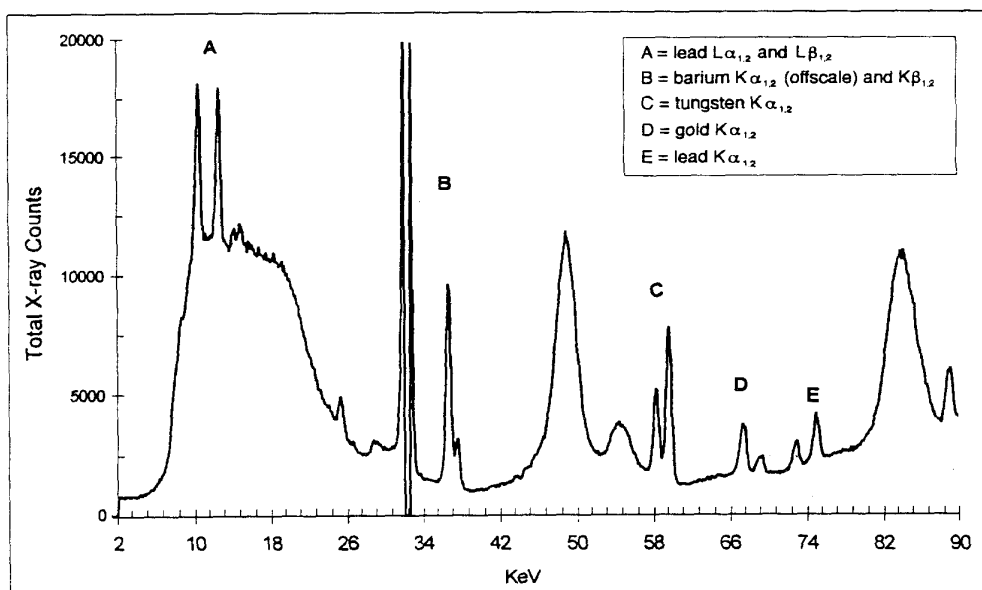


Figure 1. XRF spectrum of 1.02 mg/cm² NIST paint on wallboard.

7.1.2. Detector Response

The response of the Si(Li) detector varies with different X-ray energies and is optimal at wavelengths greater than 0.4 angstroms. Differences in the response of the Si(Li) detector for lead K- and L-line X-rays were estimated using the ratio of the integrated Lⁿ/Kⁿ₁ and Lⁿ/Kⁿ₁ X-ray peaks for each of the lead concentrations of the NIST paint SRM (Table 3). At the action level of 1.0 mg/cm² lead, the Si(Li) detector demonstrated twice the response to the lead L-line versus K-line X-rays. The increased response of the Si(Li) detector to L-line X-rays was offset by the large scatter band or background continuum extending from 6.0 to 24.0 KeV. In the L-line region of the spectrum, 61% of the X-ray counts resulted

from this background continuum. The scatter is presumably caused by the high-energy Co⁵⁷ source, which excites elements such as tungsten (from shielding material in the detector) and barium (in the paint matrix) that emit K-line and other scatter X-rays with sufficient energies to excite the other elements in turn. The phenomenon is similar to an X-ray tube in direct mode. The source-detector geometry of the field XRF appears to promote background scatter.

Table 3. The HNu Si(Li) detector response to Pb K- and L-line X-rays.

Lead Conc. (mg/cm ²)	K α_1 Integrated CPS	L α Integrated CPS	Ratio L α /K α_1	K α_2 Integrated CPS	L β Integrated CPS	K α_1 Integrated CPS
0.29	27.88	32.88	1.18	10.69	30.27	2.83
1.02	44.77	106.9	2.39	26.26	105.6	4.02
1.63	62.28	150.5	2.42	31.96	154.9	4.85
3.53	107.6	290.4	2.70	63.44	313.9	4.95

An estimate of the signal-to-noise can be made using counting statistics^{11,12}, where the square root of the average number of counts is equal to the standard deviation (:) and the average number of counts is obtained from replicate measurements. When the total number of counts (N) in each measurement is large, N can be substituted for the averaged count number. The signal-to-noise ratio for a given lead line can be estimated by using the net peak counts for the lead line and dividing by the square root of the total number of counts, with background, for the peak of interest. For the lead L" X-ray line, the signal-to-noise ratio is estimated to be 86 to 1.

7.1.3. Gold External Standard

Inspection of an XRF spectrum with no gold film present (Figure 1) shows gold (D) K" ₁ (68.79 KeV) and K" ₂ (66.98 KeV) X-ray lines from excitation of gold in the Si(Li) detector. The gold K" ₁ and K" ₂ X-ray lines are overlapped by the weaker tungsten K\$₁ (67.23 KeV) and K\$₂ (69.09 KeV) X-rays generated by the tungsten shielding around the source, causing the change in the peak heights of the gold K-line X-rays. Because this background is constant, only the instrument detection limit and sensitivity to added gold foil are reduced. This loss in sensitivity was offset by adding the gold K" ₁ and K" ₂ integrated peak areas to evaluate the combined total gold counts per second (cps) as demonstrated in the XRF spectrum of the 1.02-mg/cm² paint SRM (Figure 2) with the 49.48-m² gold foil placed behind the paint SFW. The gold K" x-ray lines (D) are distinct and free of Co⁵⁷ scatter interferences. In the presence of the large gold external standard, the gold K\$₁ line (F, 77.97 KeV) is also observable.

Inspection of the L-line region of the paint SRM with the large gold external standard (Figure 2) shows that the detector-MCA combination in the field XRF system is insufficient to resolve the L-lines of lead and gold from each other (A). The gold L" _{1,2} lines (9.71,9.63 KeV, respectively) are buried in the scatter peak on the left side of the lead L" _{1,2} lines (10.55, 10.45 KeV, respectively). The gold L\$_{1,2} lines (11.44, 11.58 KeV, respectively) are midway between and overlapped by the taller lead L" _{1,2} and L\$_{1,2} (12.61, 12.62 KeV, respectively) lines. Because of this lack of resolution and the large scatter band under the L-line region in the field XRF instrument, subsequent L-line studies were restricted to the laboratory XRF instrument.

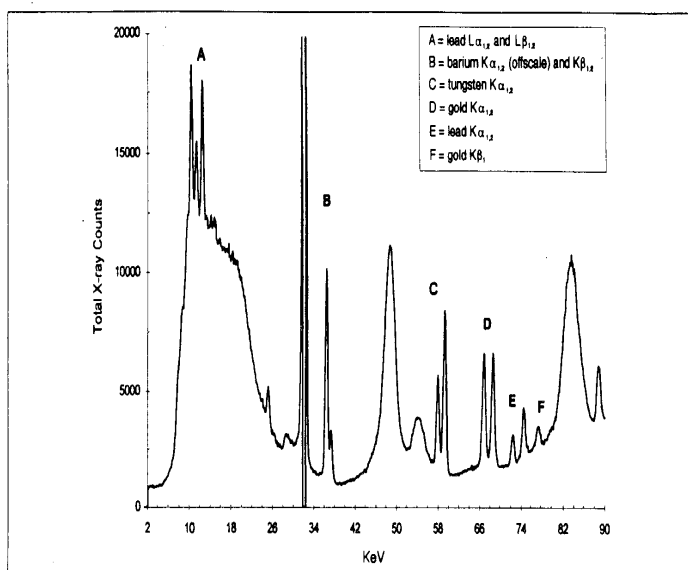


Figure 2. XRF spectrum of 1.02 mg/cm² NIST paint with gold disk on wallboard.

Neither of the gold external standards had an effect on the conventional calibration curve for lead as evidenced by nearly equal slopes, y-intercepts, and correlation coefficients obtained for each test condition (Table 4). By inspection, the gold counts also are unaffected by the changing lead concentrations in the paint SRMs (Fig. 3).

Table 4. Data showing the gold external standard effects on lead calibration data.

X-ray line ID	Gold Area (mm ²)	Slope (cps/mm ²)	Y-Intercept	Correlation Coefficient
Lead K α_1	0.00	136	90.1	0.9995
Lead K α_1	7.92	132	92.2	0.9997
Lead K α_1	49.5	134	95.1	0.9997
Lead K α_2	0.00	85.8	29.6	0.9973
Lead K α_2	7.92	83.0	37.4	0.9974
Lead K α_2	49.5	85.4	36.8	0.9995

The minimum area for the gold foil was defined as the area of foil which results in an integrated counts/second (cps) three sigma above the average gold background cps (from the detector alone) using the combined gold K α_1 and K β_1 peak area counts from each paint SRM used in a lead calibration curve. The average background value of 85.0 cps and a sigma value of ± 3.8 cps was determined. The minimum gold external standard area was calculated to correspond to $85.0 + 3 \times 3.8 = 96.4$ cps. From a plot of the average gold cps of the 7.92 and 49.48 mm² gold external standards versus gold surface area, the minimum area of gold was calculated to be 3.42 mm². In this application of statistics to the analysis of counting-rate errors, the three-sigma value ensures (with greater than 99% certainty) that the variation in gold cps between the background and with the minimum area of gold present represents a true difference in populations.¹³

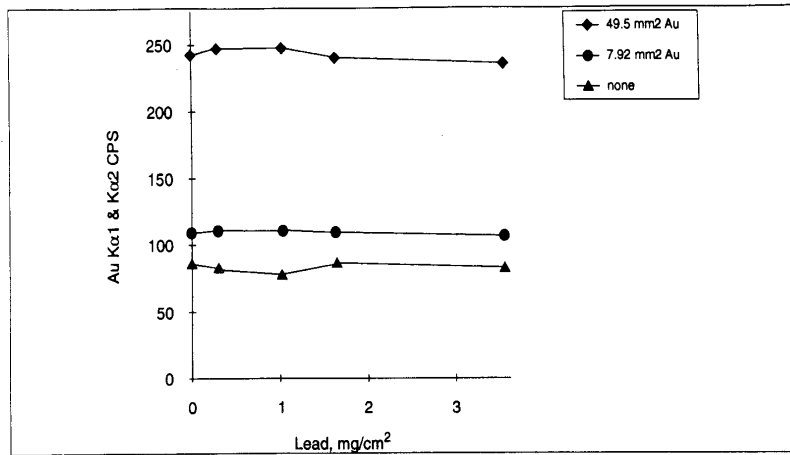


Figure 3. Gold counts are unaffected by the changing concentration of the paint SRMs.

7.1.4. Titanium Foil Cover-layers

The titanium K-line X-rays were so low in energy that detection by the field XRF instrument was unattainable. To verify that there was no shielding effect on intensities related to lead concentrations, the complete set of paint SRMs was analyzed for each thickness of titanium-foil coverlayer. For a given thickness of titanium, the slopes for each calibration curve, using the lead K₁ X-ray line, were equivalent (within experimental error) to the calibration values obtained when no titanium coverlayer was present (Table 5). Measurements were also performed in triplicate (the titanium-free sample was analyzed 4 times) using the 1.02 mg/cm² paint SRM with each different thickness of titanium foil. Even the thickest (0.081 mm) titanium foil caused so little attenuation of the lead and gold X-rays as to be indistinguishable from measurements taken with no titanium foil present. Examination of the average values of the lead K₂ and the combination of K₁ and K₂ gold X-rays indicated no effect from the titanium foil coverlayers.

Table 5. Lead calibration and replicate analysis data in the presence of titanium coverlayers.

Lead K _α , Calibration Curve No.	Titanium Thickness (mm)	Slope counts*cm ² mg*sec	Correlation Coefficient	Replicates	Average & SD Replicates (K _α , cps)
1	none	26.47	0.999	4	46 ± 2
2	0.025	26.57	0.998	3	47 ± 2
3	0.050	24.09	0.999	3	46 ± 1
4	0.081	26.12	0.999	3	45 ± .3

7.2. Laboratory XRF

Data for all experiments performed with the laboratory XRF instrument on lead paint alone or in combination with gold, titanium, or plastic film are listed in Table 2 in the Appendix. The laboratory XRF instrument resolved the L^α and L^β lines of lead and gold (Figure 4) in contrast to the incomplete resolution observed in spectra from the field XRF instrument.

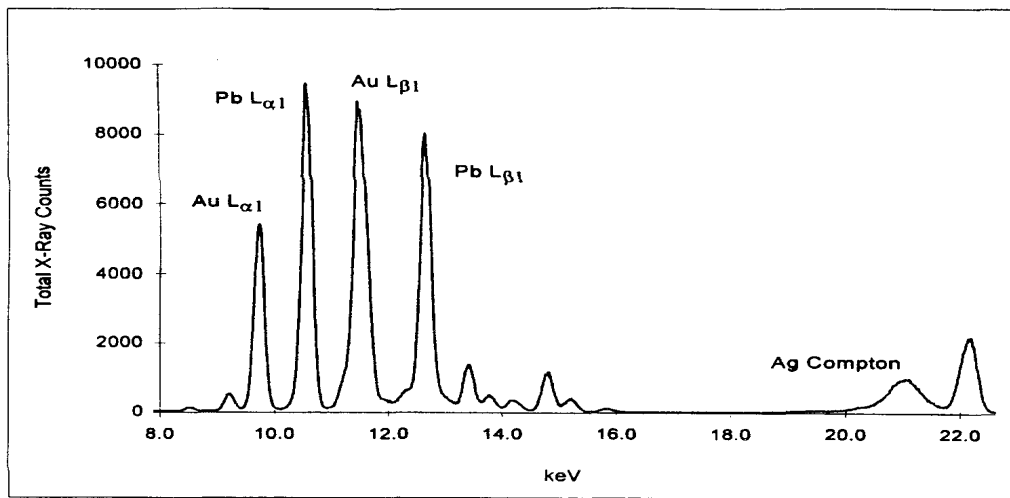


Figure 4. Laboratory XRF spectrum of 1.02 mg/cm² NIST lead-based paint with gold external standard, demonstrating complete resolution of lead and gold X-rays.

The lead L β line was used for quantitation because slightly higher count rates were achieved versus the L α line, and the L β line was free from any presence of arsenic. Similar values for the slopes of the lead calibration line were obtained in the presence (1145 cps/mg/cm²) and absence (1186 cps/mg/cm²) of the gold external standard demonstrating that the gold external standard had little or no effect on the calibration curve for lead. However, both curves did demonstrate a loss of linearity at 3.53 mg/cm² lead, as is shown by the dotted line in Figure 5. The high lead content self-absorbs some of the fluorescent lead X-rays, preventing them from reaching the detector, and results in a decreasing average response factor even as the concentration of lead increases. The linear range of the lead calibration curve was extended by using the ratio of the lead L β line and the silver Compton scatter X-rays versus lead concentration, as shown by the solid line in Figure 6, with a slope equal to 2.12 cm²/mg. The Compton scatter correction adjusts for the nonlinear increase in counts as the concentrations of heavy metals in a sample increase.

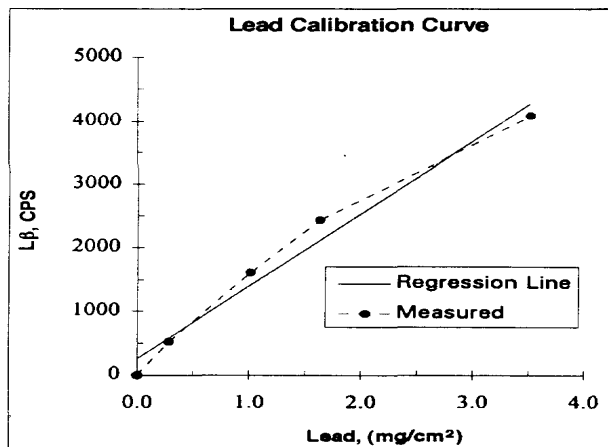


Figure 5. Saturation of XRF lead L β X-rays are observed at high lead concentrations.

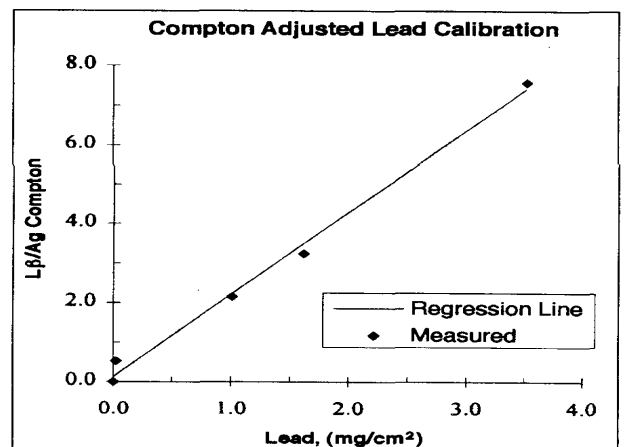


Figure 6. Lead calibration curve with lead L β /Ag Compton ratio versus concentration.

7.2.1. Metal Foil and Plastic Film Coverlayers

The coverlayers of titanium and aluminum foils and acetate plastic films produced similar results. Calibration for lead with one or more of these materials present as a coverlayer attenuated the lead X-rays and reduced the magnitude of the slope for a curve generated by plotting lead L β cps versus lead concentration. A plot of ratio of the lead L β cps and the silver Compton scatter cps versus lead concentration gave the results shown in Table 6.

Using the Compton scatter correction yielded lead calibration curves with correlation coefficients (r) greater than 0.99 for lead concentrations extending from 0.0 to 3.5 mg/cm² lead. Each material attenuated the lead L β line proportionally to the magnitude of the mass absorption coefficient and the thickness of the cover material. Generally, as the effective atomic number of the material increased, so did its ability to absorb the lead L-line X-rays. For each type of material, increasing the coverlayer thickness proportionally decreased the average counts at each point of the linear calibration curve.

Table 6. Lead calibration data in the presence of metal and plastic cover materials, using the ratio of the silver Compton and lead L β counts to extend the linear range of the calibration.

Cover material	Film Thickness (mm)	Slope cm ² mg	Cover material	Film Thickness (mm)	Slope cm ² mg	Cover material	Film Thickness (mm)	Slope cm ² mg
none	na	2.12	none ¹	na	2.16	acetate	0.356	0.577
Ti	0.006	1.60	Al	0.05	1.07	acetate	.593	0.348
Ti	0.025	0.382	Al	0.10	0.590	acetate	.830	0.248
Ti ¹	0.025	0.356	Al	0.13	0.442	B ²		0.367
Ti	0.050	0.079	Al	0.15	0.357	Ti +B ²	0.025 Ti	0.121

¹ Gold film not present.

² B is NIST paint blank cover layer. Cross section not determined because material was a mixture.

Effects of increasing the thickness of titanium foil above each sheet of the paint SRM are presented in Figure 7. The heavy solid line represents the usual calibration curve obtained using the ratio of the lead L β and the Compton scatter peaks versus the lead with no titanium present. This is the typical calibration plot obtained for the XRF determination of lead. The unevenly dashed line represents a lead calibration curve for a titanium coverlayer 0.006 mm in thickness, the equivalent of several titanium oxide paint layers covering an older lead-based paint. The thin solid line represents a lead calibration curve for a titanium coverlayer 0.025 mm in thickness, and the evenly dashed line represents a calibration curve for lead for a titanium coverlayer 0.050 mm in thickness. The ratio change of the lead L β and Compton scatter cps versus lead concentration in the 0.050-mm layer is almost indistinguishable from background noise. A titanium foil thickness greater than 0.050 mm reduces the sensitivity of the XRF measurements for lead to zero, resulting in a false negative for lead, regardless of the lead concentration beneath the titanium coverlayer or its equivalent oxide layer.

The false negative resulting from a 0.025-mm titanium coverlayer is demonstrated in Figure 7. A concentration of 5.25 mg/cm² lead in the covered paint sample is necessary to achieve the same intensity (y

axis) value that a 1.0-mg/cm² uncovered lead paint sample yields. The titanium coverlayer causes the normally calibrated XRF instrument to read 81% below the actual lead paint concentration. In the case of 0.006-mm titanium equivalents of paint covering a 1.0-mg/cm² lead-based paint layer, a reading of 0.78 mg/cm² lead is obtained, which is 22% below the actual lead concentration. The aluminum and plastic coverlayers demonstrated similar but less pronounced results (see Appendix) due to their smaller mass absorption coefficients. These examples demonstrate the introduction of false negatives into lead determinations by XRF. Also, typical QC measures, such as the continuing calibration verification and sample duplicates, do not address this type of error and are not sufficient to ensure that the data quality objectives for accuracy are met.

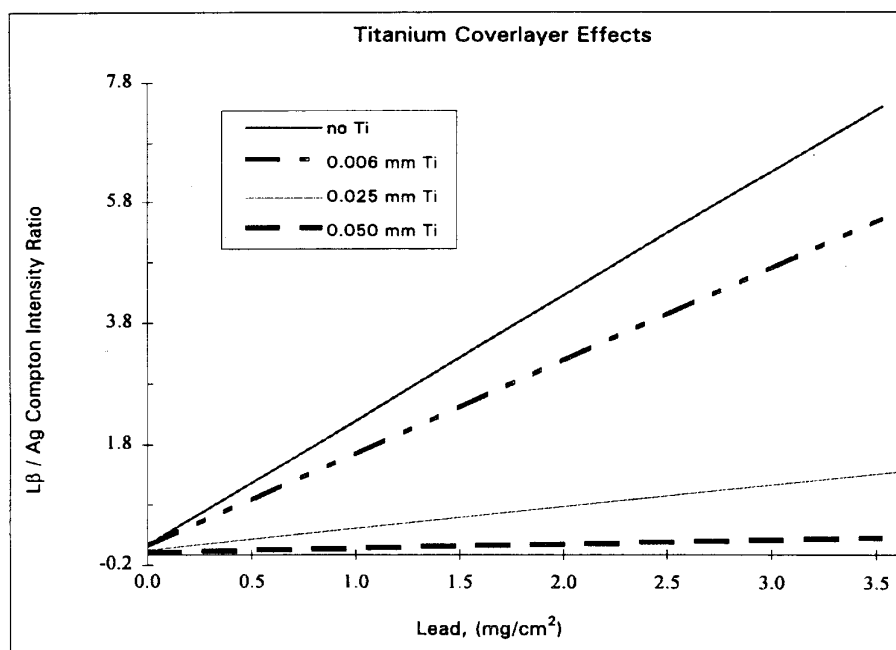


Figure 7. Titanium coverlayers reduce sensitivity of XRF to changes in lead concentration.

The accuracy of the XRF lead determinations can be increased by generating lead calibration curves using titanium covers on paint SRMs equivalent to the paint covering to be analyzed. However, this approach is only valid while the thickness of the standard and sample coverlayers remain constant. Alternatively, the gold external standard could be used to provide an indication of the extent of shielding by the coverlayers and could provide a correction for them.

7.2.2. Application of the Gold External Standard

As the thickness and mass absorption coefficient of materials covering the lead-based paint layers increase, similar reductions in gold L^α and L^β X-ray intensities are observed as for lead lines. Although the gold external standard area is constant, different X-ray counts are obtained depending on the type and thickness of the covering materials as well as the lead paint. The extent of this shielding is dependent on the concentration (thickness) of the lead paint layer. Changes in intensity of the gold X-rays alone do provide useful information other than an indication that the XRF is operating properly. Figure 8 demonstrates the

changes in the L-line spectra of lead and gold as titanium coverlayers of increasing thickness are added above on top of the lead paint layer.

Closer inspection of Figure 8 reveals that changes in peak heights of the lead and gold L β lines are not equivalent to those observed for the L α lines as the thickness of the titanium cover-layer is increased. The L α line, which is further from the silver source X-rays, decreases more rapidly than the L β lines. Therefore, it is the ratio of the L β /L α gold and lead X-rays that increases as the thickness of the titanium coverlayer is increased. It is this phenomenon that is exploited for quantitative determinations on thin film samples.¹⁴

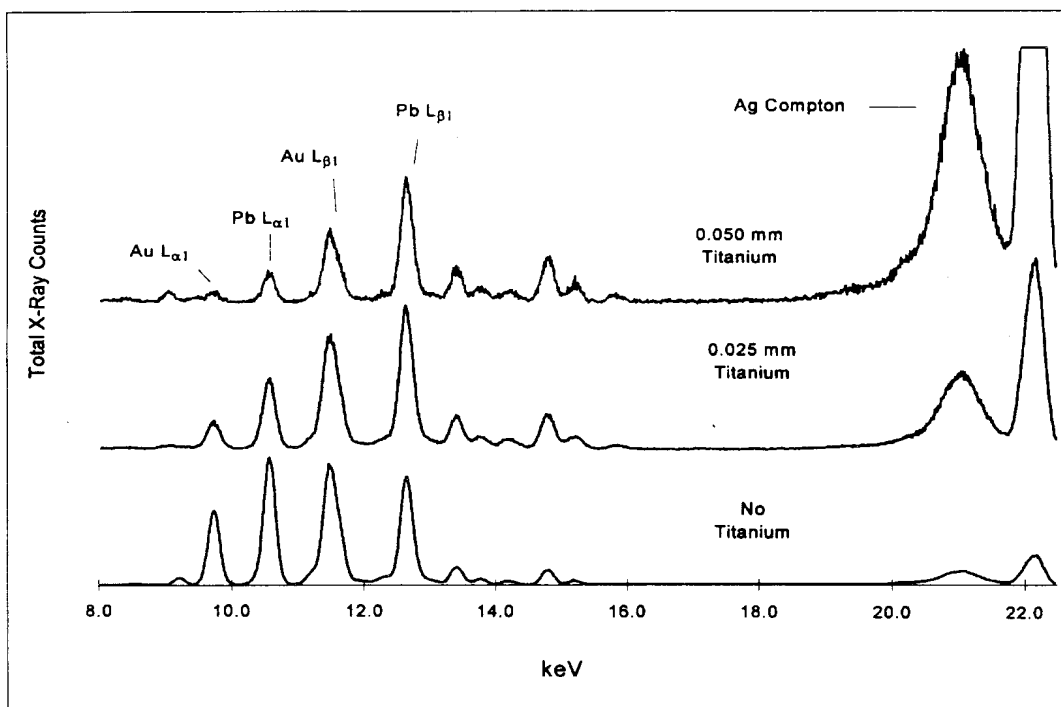


Figure 8. Relative peak height differences of gold and lead L-line X-rays with increasing thickness of titanium coverlayers over lead-based paint using silver X-rays for excitation.

The relationship between peak heights and titanium coverlayer thickness is shown in Figure 9. For this work, it is assumed that the lead layer or layers are located immediately above the gold external standard. The titanium thickness is the actual path transversed by the silver X-rays in and the lead X-rays out through the titanium cover-layer, consistent with an X-ray source and detector at an angle 45 $^{\circ}$ incident to the paint surface. Figure 9 shows the change in the gold L β /L α ratio for each sample of the paint SRM with increasing titanium coverlayer thickness, where each line represents the gold L-line ratio for one sample of the paint SRM. The change in the gold L-line ratio appears to be independent of the lead concentration. In the case of titanium, the correlation coefficients for the gold L-line ratio versus thickness had values of 0.98 or greater. The average regression line of the five paint SRMs has a value of 100 \pm 10 mm $^{-1}$.

The values for aluminum and plastic are listed in Table 7 and are shown in Appendix figures A1 and A2. Table 7 shows that the slope or rate of change of gold L β /L α ratio versus coverlayer thickness is dependent

on the mass absorption coefficient of the cover material. The material that has the largest mass absorption coefficient has the steepest slope, in this case titanium, followed by aluminum and then plastic. A similar trend is also observed for the lead $L\beta/L\alpha$ line ratios as shown in Figure 10. However, the trend for increasing line ratios with increasing coverlayer thickness appears linear only for very thin coverlayers.

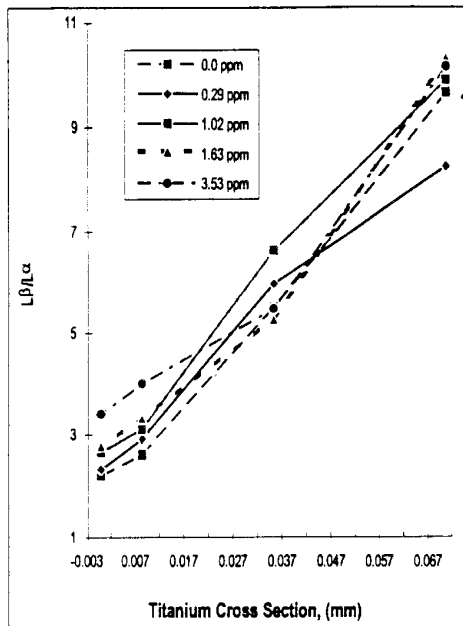


Figure 9. Effect of titanium coverlayers on gold $L\beta/L\alpha$ X-ray line ratios.

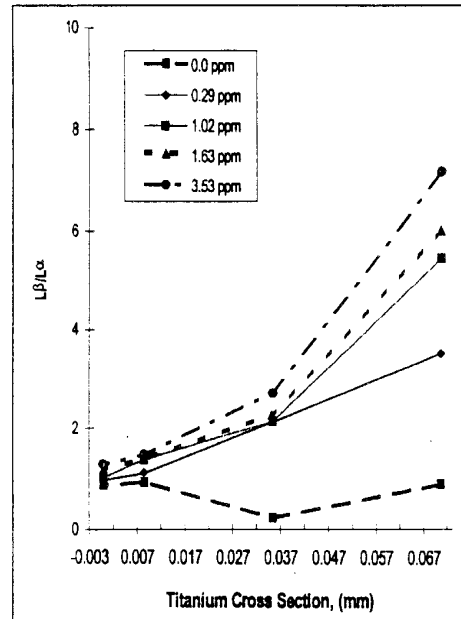


Figure 10. Effect of titanium coverlayers on lead $L\beta/L\alpha$ X-ray line ratios.

If an XRF measurement is made of a paint surface to which a gold external standard has been applied, the average slope can potentially be used with the experimentally measured gold L-line ratio to estimate the thickness of a coverlayer over a lead-based paint in terms of titanium equivalents. This information can then be used to calculate the corrected intensity for the lead L-lines as if no coverlayer was present. The general expression which must account for changes in the coverlayer mass absorption will be completed in Phase III.

Table 7. Rate changes of gold $L\beta/L\alpha$ line ratio versus coverlayer thickness.

SRM	Titanium			Aluminum			Plastic		
	Conc. (mg/cm ²)	Slope (mm ⁻¹)	r	Y*	Slope (mm ⁻¹)	r	Y*	Slope (mm ⁻¹)	r
0.00	108	0.997	1.9	9.3	0.994	2.1	0.34	0.973	2.2
0.29	86.3	0.991	2.4	9.8	0.999	2.3	0.42	0.835	2.3
1.02	106	0.996	2.5	13.2	0.991	2.5	0.53	0.973	2.6
1.63	107	0.984	1.7	13.7	0.994	2.7	0.60	0.998	2.8
3.53	94	0.979	3.1	15.7	0.985	3.3	0.57	0.964	3.4
Avg. Slope	100 ±10			12.3 ±2.7			0.49 ±0.11		

*Y= value for the Y intercept

8. Summary

Current XRF measurement techniques are subject to substrate and matrix effects which can result in either an over- or under-estimation of the lead concentration. The goal of this feasibility study was to evaluate if analytical protocols for lead determinations by XRF could be developed that use an insertable external standard to eliminate false negatives in lead detection and increase the accuracy of the quantitative results.

False-negative conditions for K- and L-line X-rays were simulated using titanium, aluminum, and acetate-film cover materials. Use of a gold external standard was demonstrated to be feasible with a field XRF instrument containing a high-resolution Si(Li) detector. For K-line lead determinations, the gold external standard positioned at the substrate level is a useful indicator of X-ray penetration through a multi-layered paint matrix. No correction to the lead K-line X-rays is necessary because they are unaffected by test-cover materials. The lead L-lines were sufficiently broadened by the high energy Co⁵⁷ source and instrument geometry to cause overlap with the gold L-lines of the external standard and could not be used.

The gold external standard was feasible for L-line determinations of lead using a laboratory XRF instrument which generated low-energy silver X-rays. The maximum linear range for lead calibrations was achieved using the ratio of the lead L_α and the silver Compton scatter X-rays versus lead concentration. The titanium, aluminum, and plastic cover materials were experimentally shown to be one source of false negatives for the XRF determination of lead. A gold external standard placed beneath the paint SRM was shown to be free of interferences from materials in the paint matrix and to have no effect on the lead calibration curve. The value for the ratio of the gold L_α/L_β X-rays was found to increase as the thickness of a cover material was increased. This change in the gold L_α/L_β ratio is relatively independent of lead concentration, changing only with increasing cover material thickness. The slope or rate of change of gold L_α/L_β ratio versus cover material thickness was proportional to the magnitude of the mass absorption coefficient of the cover material.

This work demonstrates that the use of a gold external standard to correct for matrix effects and eliminate one source of false negatives in the XRF determination of lead is feasible. The mass of gold external standard required was higher than expected because it was necessary to differentiate between gold X-rays from the coating on the Si(Li) detector and those from the external standard when using the high-energy Co⁵⁷ source. Further investigations should be performed to determine if an alternative external standard material such as platinum, which is uncommon in the environment and free from interference, would be suitable for use with the field XRF instrument. Studies are in progress to develop a general expression to calculate intensity corrections for the lead L-lines when cover materials are present and to account for changes in the cover material mass absorption coefficients.

9. References

1. Waldman, S., "Lead and Your Kids", *Newsweek*, July 15, 1991, pp. 42-47.
2. Vincent, H. A., Kilduff, J. E., *Advances in the Quality Assurance for XRF Determinations of Lead in Painted Surfaces and In Soils*, 43rd Annual Denver X-Ray Conference, Steamboat Springs, Colorado, August 1994.
3. Vincent, H. A., Kilduff, J. E., *Advances in the Quality Assurance for XRF Determination of Lead in Painted Surfaces*, Tenth Annual Waste Testing and Quality Assurance Symposium, Washington D. C., July 1994.
4. Raspberry, S. D., "Investigation of Portable X-ray Fluorescence Analyses for Determining Lead on Painted Surfaces": *Applied Spectroscopy*, Vol. 27, No. 2. 1973.
5. Personal Communication, H. A. Vincent and L. R. Williams, Environmental Monitoring Systems Laboratory, Office of Research and Development, U.S. Environmental Protection Agency, Las Vegas Nevada, March 1992.
6. Kilduff, J. E., "XRF Quality Assurance Study with Gold External Standard Progress Report: Phase I", EPA/600/X-94/007, Environmental Monitoring Systems Laboratory, Office of Research and Development, U.S. Environmental Protection Agency, Las Vegas, Nevada, 1993.
7. Bertin, E. P., *Principles and Practice of X-ray Spectrometric Analysis*, Second Edition, Plenum Press, New York, 1975, pp. 613-615.
8. Bruno, J. A., Appleman, B. R., "Developing and Evaluating Environmentally Acceptable Coatings", *Journal of Protective Coatings and Linings*, November, 1984.
9. Pella, P. A., McKnight, M., Murphy, K. E., Vocke, R. D., Byrd, E., DeVoe, J. R., Kane, J. S., Lagergren, E. S., Schiller, S. B., and Marlow A. F., "NIST-SRM 2579 Lead Paint Films for Portable X-Ray Fluorescence Analyzers", contract no. IAG DU-100191-0000026, National Institute of Standards and Technology, Gaithersburg, MD, 1992, pp. 2-4.
10. Jenkins, R., Gould, R. W., Gedcke, D., *Quantitative X-ray Spectrometry*, Marcel Dekker, Inc., New York, 1981, pp. 205-206.
11. Bertin, E. P., *Principles and Practice of X-Ray Spectrometric Analysis*, Second Edition, Plenum Press, New York, 1975, p. 250.
12. Tertian, R., Claisse, F., *Principles of Quantitative X-Ray Fluorescence Analysis*, Heyden Press, London, 1982, pp. 334-345.
13. Chase, G., D., Rabinowitz, J. L., *Principles of Radioisotope Methodology*, Burgess Publishing Co., Minneapolis, Minnesota, 1967, pp. 95-97.
14. KeveX Instruments, *KeveX XRF Toolbox II Reference Manual*, P/N 7180-5060, January 1990, pp. 2-68, 2-77.

APPENDIX

Definitions □

Ag Compton Area - silver Compton scatter X-ray line intensities from inelastically scattered X-rays from a secondary silver target measured in counts per second (cps).

Ag Compton / Raleigh Ratio - silver Compton scatter X-ray line intensities (inelastic scatter) over silver Raleigh scatter X-ray line intensities (elastic scatter).

Au L^α - gold L^α X-ray line intensities measured in cps.

Au L_β - gold L_β X-ray line intensities measured in

Au L_β /Ag Compt - ratio of gold L_β X-ray line intensities over silver Compton scatter X-ray line intensities.

coverlayer - the metal foil or plastic film layer of material placed over a paint SRM to simulate new paints over older, lead-based paint.

cps - counts per second are units for quantification of X-ray line intensities.

Integrated Area - silver Compton scatter X-ray line intensities measured in cps in the interval 20.08 KeV

Pb L^α - gold La X-ray line intensities measured in cps.

Pb L_β - gold L_β X-ray line intensities measured in cps.

Pb L_β /Ag Compt - ratio of lead L_β X-ray line intensities over silver Compton scatter X-ray line intensities.

Table A1. Field XRF data obtained with paint SRMs, titanium foil covers and gold external standard.

Spectra ID	Lead Conc. mg/cm ²	Gold Area (mm)	Film ID & Thickness (mm)	Livetime (sec)	Actual Time (sec)	Source Activity (%)	Measured & Calculated Variables					
							Pb K α 1 (cps)	Pb K α 2 (cps)	Au K α 1,2 (cps)	Au K β 1 (cps)	Pb K α 1 / Pb K α 2	Au K α 1,2 / Pb K α 1
1	0.00	0.00	none	74.3	301.55	84	16.9	5.1	87.4	nd	3.31	5.2
2	0.29	0.00	none	74.3	301.55	84	27.7	10.6	84.8	nd	2.61	3.1
3	1.02	0.00	none	74.4	301.69	84	44.2	26.1	78.9	nd	1.69	1.8
4	1.63	0.00	none	74.3	301.63	84	61.9	31.8	88.6	nd	1.95	1.4
5	3.53	0.00	none	74.3	301.77	84	113.6	66.2	85.5	nd	1.72	0.8
6	0.00	7.92	none	74.3	302.41	85	17.4	7.5	111.4	nd	2.31	6.4
7	0.29	7.92	none	na	302.15	85	25.5	10.6	112.4	nd	2.41	4.4
8	1.02	7.92	none	74.4	302.08	85	46.2	27.0	112.8	nd	1.71	2.4
9	1.63	7.92	none	74.4	301.55	85	61.8	33.4	111.7	nd	1.85	1.8
10	3.53	7.92	none	74.3	301.12	85	110.2	65.7	108.8	nd	1.68	1.0
11	0.00	49.48	none	74.1	300.89	86	19.1	8.4	243.4	22.51	2.28	12.7
12	0.29	49.48	none	74.0	300.73	86	26.1	11.3	248.3	21.38	2.30	9.5
13	1.02	48.48	none	74.0	300.03	86	47.8	24.3	248.0	20.75	1.97	5.2
14	1.02	49.48	none	74.1	300.64	86	43.9	23.0	251.5	20.05	1.90	5.7
15	1.02	49.48	none	74.1	300.60	86	48.0	24.0	249.8	23.83	2.00	5.2
17	1.02	49.48	none	74.1	300.52	86	44.8	23.1	251.0	20.93	1.94	5.6
18	1.63	49.48	none	73.9	304.12	86	60.9	35.1	242.4	19.03	1.73	4.0
19	3.53	49.48	none	73.8	303.51	86	112.6	66.9	238.4	18.65	1.68	2.1
20	0.00	49.48	0.025 Ti	74.3	301.33	86	16.4	5.3	230.1	18.62	3.13	14.0
21	0.29	49.48	0.025 Ti	74.2	301.25	86	25.6	13.0	238.2	20.71	1.97	9.3
22	1.02	49.48	0.025 Ti	74.2	300.01	86	48.3	25.7	241.2	22.30	1.88	5.0
23	1.02	49.48	0.025 Ti	74.3	301.18	86	47.6	24.4	236.6	22.21	1.95	5.0
24	1.02	49.48	0.025 Ti	74.2	301.44	86	44.6	22.8	241.0	21.90	1.96	5.4
25	1.63	49.48	0.025 Ti	74.1	300.73	86	60.8	33.2	242.8	17.65	1.83	4.0
26	3.53	49.48	0.025 Ti	74.0	300.43	86	111.5	66.7	243.4	15.59	1.67	2.2

nd = not determined

na = not available

Table A1. Field XRF data obtained with paint SRMs, titanium foil covers and gold external standard (continued).

Spectra ID	Lead Conc. mg/cm ²	Gold Area (mm)	Film ID & Thickness (mm)	Livetime (sec)	Actual Time (sec)	Source Activity (%)	Calculated Variables					
							Pb K α 1 (cps)	Pb K α 2 (cps)	Au K α 1&2 (cps)	Au K β 1 (cps)	<u>Pb Kα1</u> / <u>Pb Kα2</u>	<u>Au Kα1,2</u> / <u>Pb Kα1</u>
27	0.00	49.48	0.050 Ti	74.2	301.17	86	18.0	7.9	242.2	19.69	2.27	13.4
28	0.29	49.48	0.050 Ti	74.2	301.01	86	26.3	12.7	241.3	20.22	2.08	9.2
29	1.02	49.48	0.050 Ti	74.2	301.36	86	44.8	23.1	239.6	21.12	1.94	5.3
30	1.02	49.48	0.050 Ti	74.2	301.26	86	46.6	23.9	231.5	20.90	1.95	5.0
31	1.02	49.48	0.050 Ti	74.3	301.41	86	45.3	21.7	232.3	17.58	2.09	5.1
32	1.63	49.48	0.050 Ti	74.2	301.26	86	60.3	33.0	236.8	17.39	1.83	3.9
33	3.53	49.48	0.050 Ti	74.2	300.97	86	103.8	57.0	222.3	14.60	1.82	2.1
34	0.00	49.48	0.081 Ti	74.3	301.75	86	16.5	4.8	244.9	20.39	3.46	14.9
35	0.29	49.48	0.081 Ti	74.2	300.30	86	26.3	10.6	241.9	19.36	2.47	9.2
36	1.02	49.48	0.081 Ti	74.2	300.30	86	45.4	21.8	236.0	18.28	2.08	5.2
37	1.02	49.48	0.081 Ti	74.2	300.94	86	45.1	23.6	239.4	19.87	1.91	5.3
38	1.02	49.48	0.081 Ti	74.2	300.93	86	45.7	21.0	239.1	20.93	2.18	5.2
39	1.63	49.48	0.081 Ti	74.2	300.93	86	59.7	32.3	232.3	16.23	1.85	3.9
40	3.53	49.48	0.081 Ti	74.1	300.94	86	110.0	63.6	235.5	17.12	1.73	2.1
41	none	0.00	none	74.8	303.42	86	16.5	6.4	91.0	0	2.59	5.5

nd = not determined

na = not available

Table A2. Laboratory XRF data obtained with lead paint SRMs, film coverlayers and gold external standard.

Spectra ID	Lead Conc. mg/cm ²	Film ID & Thickness (mm)	Measured Variables					Calculated Variables						
			Au Lβ	Au Lα	Pb Lβ	Pb Lα	Ag Cmp	Pb Lβ	Au Lβ	Ln ()		Au Lβ	Pb Lβ	Au Lβ
			(cps)	(cps)	(cps)	(cps)	(cps)	Ag Cmpt	Ag Cmpt	Au LB	Au Lα	Au Lα	Pb Lα	Pb Lβ
1	0.00	0.05 Ti + Au	58	6.0	1	1	669	9.05e-04	8.74e-02	4.07	1.80	9.68	0.92	96.5
2	0.29	0.05 Ti + Au	48	5.7	17	5	647	2.65e-02	7.35e-02	3.86	1.75	8.27	3.56	2.77
3	1.02	0.05 Ti + Au	39	4.0	60	11	612	9.78e-02	6.43e-02	3.67	1.38	9.93	5.49	0.66
4	1.63	0.05 Ti + Au	37	3.5	99	16	618	1.61e-01	5.91e-02	3.60	1.26	10.36	6.05	0.37
5	3.53	0.05 Ti + Au	25	2.5	195	27	699	2.79e-01	3.59e-02	3.22	0.90	10.19	7.21	0.13
6	0.00	0.025 Ti + Au	360	65.1	0	2	766	5.27e-04	4.70e-01	5.89	4.18	5.52	0.24	891
7	0.29	0.025 Ti + Au	375	62.7	103	48	758	1.36e-01	4.95e-01	5.93	4.14	5.99	2.14	3.65
8	1.02	0.025 Ti + Au	333	50.1	323	150	684	4.71e-01	4.86e-01	5.81	3.91	6.64	2.15	1.03
9	1.63	0.025 Ti + Au	197	37.3	395	172	676	5.85e-01	2.91e-01	5.28	3.62	5.28	2.29	0.50
10	3.53	0.025 Ti + Au	133	24.2	753	275	547	1.38e+00	2.43e-01	4.89	3.19	5.49	2.74	0.18
11	0.00	0.006 Ti + Au	1784	681.6	3	3	900	3.09e-03	1.98e+00	7.49	6.52	2.62	0.94	642
12	0.29	0.006 Ti + Au	1725	590.9	372	333	866	4.30e-01	1.99e+00	7.45	6.38	2.92	1.12	4.63
13	1.02	0.006 Ti + Au	1429	460.7	1224	881	749	1.63e+00	1.91e+00	7.27	6.13	3.10	1.39	1.17
14	1.63	0.006 Ti + Au	1219	365.8	1850	1314	753	2.46e+00	1.62e+00	7.11	5.90	3.33	1.41	0.66
15	3.53	0.006 Ti + Au	773	192.7	3188	2138	563	5.66e+00	1.37e+00	6.65	5.26	4.01	1.49	0.24
16	0.00	Au only	2479	1119	4	5	957	4.67e-03	2.59e+00	7.82	7.02	2.21	0.89	555
17	0.29	Au only	2371	1018	504	515	902	5.59e-01	2.63e+00	7.77	6.93	2.33	0.98	4.70
18	1.02	Au only	2032	762	1576	1530	780	2.02e+00	2.60e+00	7.62	6.64	2.67	1.03	1.29
19	1.63	Au only	1733	622	2484	2069	776	3.20e+00	2.23e+00	7.46	6.43	2.79	1.20	0.70
20	3.53	Au only	1078	316	4224	3285	563	7.50e+00	1.91e+00	6.98	5.76	3.41	1.29	0.26
21	0.00	none	0.6	2.4	0	0	900	4.56e-04	6.25e-04	-0.58	0.88	0.23	2.32	1.37
22	0.29	none	1.0	0.7	523	467	1011	5.18e-01	1.02e-03	0.03	-0.31	1.41	1.12	0.00
23	1.02	none	8.9	3.9	1614	1383	746	2.16e+00	1.19e-02	2.19	1.36	2.29	1.17	0.01
24	1.63	none	16.2	4.3	2435	2032	749	3.25e+00	2.17e-02	2.79	1.45	3.79	1.20	0.01
25	3.53	none	24.7	7.4	4098	3192	539	7.60e+00	4.59e-02	3.21	2.00	3.33	1.28	0.01

Table A2. Laboratory XRF data obtained with lead paint SRMs, film coverlayers and gold external standard (continued).

Spectra ID	Lead Conc. mg/cm ²	Film ID & Thickness (mm)	Measured Variables					Calculated Variables						
			Au LB	Au L α	Pb LB	Pb L α	Ag Cmp	Pb LB	Au LB	Ln ()		Au LB	Pb LB	Au LB
			(cps)	(cps)	(cps)	(cps)	(cps)	Ag Cmp	Ag Cmp	Au LB	Au L α	Au L α	Pb L α	Pb LB
26	0.00	0.025 Ti	1.2	3.3	0.3	0.6	865	3.95e-04	1.39e-03	0.185	1.20	0.362	0.574	3.521
27	0.29	0.025 Ti	0.6	1.0	103.7	42.4	901	1.15e-01	6.42e-04	-0.547	-0.042	0.603	2.45	0.006
28	1.02	0.025 Ti	1.9	5.0	337.6	136.7	776	4.35e-01	2.41e-03	0.624	0.33	1.34	2.47	0.006
29	1.63	0.025 Ti	0.9	0.3	445.7	177.7	626	7.12e-01	1.41e-03	-0.124	-1.26	3.12	2.51	0.002
30	3.53	0.025 Ti	0.3	1.1	762.2	271.8	609	1.25e+00	4.60e-04	-1.27	0.115	0.250	2.80	0.000
31	0.29	0.025 Ti, B ¹ + Au	113	16.6	38	10	1115	3.43e-02	1.01e-01	4.72	2.81	6.78	3.94	2.939
32	1.02	0.025 Ti, B ¹ + Au	106	16.0	143	43	1067	1.34e-01	9.92e-02	4.66	2.77	6.62	3.32	0.739
33	1.63	0.025 Ti, B ¹ + Au	93.2	14.9	213	64	847	2.52e-01	1.10e-01	4.53	2.70	6.25	3.31	0.437
34	3.53	0.025 Ti, B ¹ + Au	51.5	8.4	355	98	823	4.31e-01	6.26e-02	3.94	2.13	6.13	3.61	0.145
35	0.29	B ¹ + Au	857	233	205	138	1564	1.31e-01	5.48e-01	6.75	5.45	3.67	1.48	4.188
36	1.02	B ¹ + Au	732	170	667	415	1466	4.55e-01	5.00e-01	6.60	5.14	4.30	1.61	1.098
37	1.63	B ¹ + Au	611	135	969	577	1427	6.79e-01	4.28e-01	6.41	4.91	4.51	1.68	0.630
38	3.53	B ¹ + Au	396	67.4	1698	946	1270	1.34e+00	3.11e-01	5.98	4.21	5.87	1.79	0.233
39	0.00	0.15 Al + Au	729	172	0.9	0.2	1387	6.13e-04	5.26e-01	6.59	5.15	4.23	4.04	858
40	0.29	0.15 Al + Au	685	155	169	102	1330	1.27e-01	5.15e-01	6.53	5.04	4.42	1.66	4.04
41	1.02	0.15 Al + Au	577	106	551	298	1257	4.39e-01	4.59e-01	6.36	4.66	5.45	1.85	1.05
42	1.63	0.15 Al + Au	453	80	789	425	1256	6.28e-01	3.61e-01	6.12	4.38	5.66	1.86	0.575
43	3.53	0.15 Al + Au	320	49.7	1453	708	1141	1.27e+00	2.81e-01	5.77	3.91	6.44	2.05	0.220
44	0.00	0.13 Al + Au	862	228	0.6	0.5	1300	4.59e-04	6.63e-01	6.76	5.43	3.78	1.24	1443
45	0.29	0.13 Al + Au	827	201	206	135	1314	1.57e-01	6.29e-01	6.72	5.30	4.12	1.53	4.02
46	1.02	0.13 Al + Au	713	144	658	392	1202	5.48e-01	5.93e-01	6.57	4.97	4.96	1.68	1.08
47	1.63	0.13 Al + Au	545	104	914	542	1197	7.64e-01	4.56e-01	6.30	4.64	5.25	1.69	0.596
48	3.53	0.13 Al + Au	350	53.7	1676	889	1061	1.58e+00	3.30e-01	5.86	3.98	6.52	1.89	0.209

¹The designation B represents the paint blank in the paint SRM series used as a coverlayer.

Table A2. Laboratory XRF data obtained with lead paint SRMs, film coverlayers and gold external standard (continued).

Spectra ID	Lead Conc. mg/cm ²	Film ID & Thickness (mm)	Measured Variables					Calculated Variables						
			Au Lβ	Au Lα	Pb Lβ	Pb Lα	Ag Cmp	Pb Lβ	Au Lβ	Ln ()		Au Lβ	Pb Lβ	Pb Lβ
			(cps)	(cps)	(cps)	(cps)	(cps)	Ag Cmp	Ag Cmp	Au Lβ	Au Lα	Au Lα	Pb Lα	Pb Lα
49	0.00	0.10 Al + Au	1090	321	0.6	0.3	1256	5.13e-04	8.68e-01	6.99	5.77	3.40	2.22	1692
50	0.29	0.10 Al + Au	1050	287	251	179	1234	2.04e-01	8.51e-01	6.96	5.66	3.66	1.41	4.18
51	1.02	0.10 Al + Au	884	210	792	520	1132	7.00e-01	7.81e-01	6.78	5.35	4.21	1.52	1.12
52	1.63	0.10 Al + Au	702	158	1135	720	1120	1.01e+00	6.27e-01	6.55	5.06	4.44	1.58	0.618
53	3.53	0.10 Al + Au	488	89.7	2026	1202	964	2.10e+00	5.06e-01	6.19	4.50	5.44	1.69	0.241
54	0.00	0.05 Al + Au	1677	614	3.1	4.0	1125	2.73e-03	1.49e+00	7.42	6.42	2.73	0.78	546
55	0.29	0.05 Al + Au	1541	519	519	288	1068	4.86e-01	1.44e+00	7.34	6.25	2.97	1.80	2.97
56	1.02	0.05 Al + Au	1330	405	1151	795	969	1.19e+00	1.37e+00	7.19	6.00	3.28	1.45	1.16
57	1.63	0.05 Al + Au	1139	326	1717	1159	828	2.07e+00	1.38e+00	7.04	5.79	3.50	1.48	0.663
58	3.53	0.05 Al + Au	669	161.1	2916	1906	765	3.81e+00	8.75e-01	6.51	5.08	4.15	1.53	0.230
59	0.00	0.830 P ² + Au	1474	571	3	2	3356	9.53e-04	0.439	7.30	6.35	2.58	1.43	461
60	0.29	0.830 P ² + Au	1414	484	306	264	3249	9.40e-02	0.435	7.25	6.18	2.92	1.16	4.63
61	1.02	0.830 P ² + Au	1201	364	987	777	3161	3.12e-01	0.380	7.09	5.90	3.30	1.27	1.22
62	1.63	0.830 P ² + Au	1036	296	1524	1025	3133	4.86e-01	0.331	6.94	5.69	3.50	1.49	0.680
63	3.53	0.830 P ² + Au	634	154	2650	1709	3006	8.82e-01	0.211	6.45	5.04	4.11	1.55	0.239
64	0.00	0.593 P ² + Au	1738	678	2	3	2685	8.35e-04	0.647	7.46	6.52	2.56	0.64	775
65	0.29	0.593 P ² + Au	1540	616	331	303	2629	1.26e-01	0.586	7.34	6.42	2.50	1.09	4.65
66	1.02	0.593 P ² + Au	1391	462	1170	850	2539	4.61e-01	0.548	7.24	6.14	3.01	1.38	1.19
67	1.63	0.593 P ² + Au	1190	366	1729	1239	2529	6.84e-01	0.471	7.08	5.90	3.25	1.40	0.688
68	3.53	0.593 P ² + Au	675	180	2902	2003	2346	1.24e+00	0.288	6.51	5.19	3.75	1.45	0.233
69	0.00	0.356 P ² + Au	1966	824	2	3	2004	1.17e-03	9.81e-01	7.58	6.71	2.39	0.74	835
70	0.29	0.356 P ² + Au	1919	721	404	382	1953	2.07e-01	9.83e-01	7.56	6.58	2.66	1.06	4.75
71	1.02	0.356 P ² + Au	1611	570	1355	1036	1862	7.27e-01	8.65e-01	7.38	6.35	2.83	1.31	1.19
72	1.63	0.356 P ² + Au	1384	449	2026	1538	1885	1.07e+00	7.34e-01	7.23	6.11	3.08	1.32	0.683
73	3.53	0.356 P ² + Au	840	233	3404	2451	1658	2.05e+00	5.07e-01	6.73	5.45	3.61	1.39	0.247

¹The designation B represents the paint blank in the paint SRM series used as a coverlayer.

²The designation P represents a plastic acetate film used as a coverlayer on the paint SRM..

Table A3. Laboratory XRF calibration data for paint SRMS, film coverlayers and gold external standard.

Spectra ID	Film ID & Thickness (mm)	Statistical Information					
		Calibration line slope (m)	Units	Y Intercept	Units	Correlation Coefficient	
1	0.05 Ti + Au	Pb L β =	55.357	(cps * cm ²) / mg	2.845	cps	0.999
2	0.05 Ti + Au	Pb L β / Ag =	0.079	cm ² / mg	0.010		0.993
3	0.05 Ti + Au						
4	0.05 Ti + Au						
5	0.05 Ti + Au						
6	0.025 Ti + Au	Pb L β =	206.369	(cps * cm ²) / mg	47.679	cps	0.990
7	0.025 Ti + Au	Pb L β / Ag =	0.382	cm ² / mg	0.019		0.997
8	0.025 Ti + Au						
9	0.025 Ti + Au						
10	0.025 Ti + Au						
11	0.006 Ti + Au	Pb L β =	894.288	(cps * cm ²) / mg	170.312	cps	0.991
12	0.006 Ti + Au	Pb L β / Ag =	1.601	cm ² / mg	-0.034		1.000
13	0.006 Ti + Au						
14	0.006 Ti + Au						
15	0.006 Ti + Au						
16	Au only	Pb L β =	1186.304	(cps * cm ²) / mg	223.517	cps	0.990
17	Au only	Pb L β / Ag =	2.124	cm ² / mg	-0.093		0.999
18	Au only						
19	Au only						
20	Au only						
21	none	Pb L β =	1145.137	(cps * cm ²) / mg	252.216	cps	0.988
22	none	Pb L β / Ag =	2.158	cm ² / mg	-0.085		0.999
23	none						
24	none						
25	none						

Table A3. Laboratory XRF calibration data for paint SRMS, film coverlayers and gold external standard (continued).

Spectra ID	Film ID & Thickness (mm)	Statistical Information					
		Calibration line slope (m)	Units	Y Intercept	Units	Correlation Coefficient	
26	0.025 Ti	Pb L β =	210.553	(cps * cm ²) / mg	57.463	cps	0.984
27	0.025 Ti	Pb L β / Ag =	0.356	cm ² / mg	0.042		0.993
28	0.025 Ti						
29	0.025 Ti						
30	0.025 Ti						
31	.025 Ti,B ¹ + Au	Pb L β =	94.252	(cps * cm ²) / mg	34.944	cps	0.986
32	.025 Ti,B ¹ + Au	Pb L β / Ag =	0.121	cm ² / mg	0.016		0.989
33	.025 Ti,B ¹ + Au						
34	.025 Ti,B ¹ + Au						
35	B ¹ + Au	Pb L β =	448.368	(cps * cm ²) / mg	159.483	cps	0.992
36	B ¹ + Au	Pb L β / Ag =	0.367	cm ² / mg	0.057		0.998
37	B ¹ + Au						
38	B ¹ + Au						
39	0.15 Al + Au	Pb L β =	405.617	(cps * cm ²) / mg	67.899	cps	0.994
40	0.15 Al + Au	Pb L β / Ag =	0.357	cm ² / mg	0.032		0.998
41	0.15 Al + Au						
42	0.15 Al + Au						
43	0.15 Al + Au						
44	0.13 Al + Au	Pb L β =	465.790	(cps * cm ²) / mg	88.250	cps	0.993
45	0.13 Al + Au	Pb L β / Ag =	0.442	cm ² / mg	0.038		0.998
46	0.13 Al + Au						
47	0.13 Al + Au						
48	0.13 Al + Au						

¹The designation B represents the paint blank in the paint SRM series used as a coverlayer.

Table A3. Laboratory XRF calibration data for paint SRMS, film coverlayers and gold external standard (continued).

Spectra ID	Film ID & Thickness (mm)	Statistical Information					
		Calibration line slope (m)	Units	Y Intercept	Units	Correlation Coefficient	
49	0.10 Al + Au	Pb L β =	564.455	(cps * cm ²) / mg	110.756	cps	0.992
50	0.10 Al + Au	Pb L β / Ag =	0.590	cm ² / mg	0.040		0.999
51	0.10 Al + Au						
52	0.10 Al + Au						
53	0.10 Al + Au						
54	0.05 Al + Au	Pb L β =	795.035	(cps * cm ²) / mg	232.543	cps	0.988
55	0.05 Al + Au	Pb L β / Ag =	1.068	cm ² / mg	0.131		0.996
56	0.05 Al + Au						
57	0.05 Al + Au						
58	0.05 Al + Au						
59	0.830 P ² + Au	Pb L β =	744.191	(cps * cm ²) / mg	130.893	cps	0.992
60	0.830 P ² + Au	Pb L β / Ag =	0.248	cm ² / mg	0.034		0.995
61	0.830 P ² + Au						
62	0.830 P ² + Au						
63	0.830 P ² + Au						
64	0.593 P ² + Au	Pb L β =	815.070	(cps * cm ²) / mg	172.279	cps	0.987
65	0.593 P ² + Au	Pb L β / Ag =	0.348	cm ² / mg	0.051		0.994
66	0.593 P ² + Au						
67	0.593 P ² + Au						
68	0.593 P ² + Au						
69	0.356 P ² + Au	Pb L β =	954.408	(cps * cm ²) / mg	203.170	cps	0.988
70	0.356 P ² + Au	Pb L β / Ag =	0.577	cm ² / mg	0.066		0.997
71	0.356 P ² + Au						
72	0.356 P ² + Au						
73	0.356 P ² + Au						

¹The designation B represents the paint blank in the paint SRM series used as a coverlayer.

²The designation P represents a plastic acetate film used as a coverlayer on the paint SRM..

Figure A1: Linear regression lines for varying cross-sections of aluminum covers above paint SRM versus the gold L-line ratio.

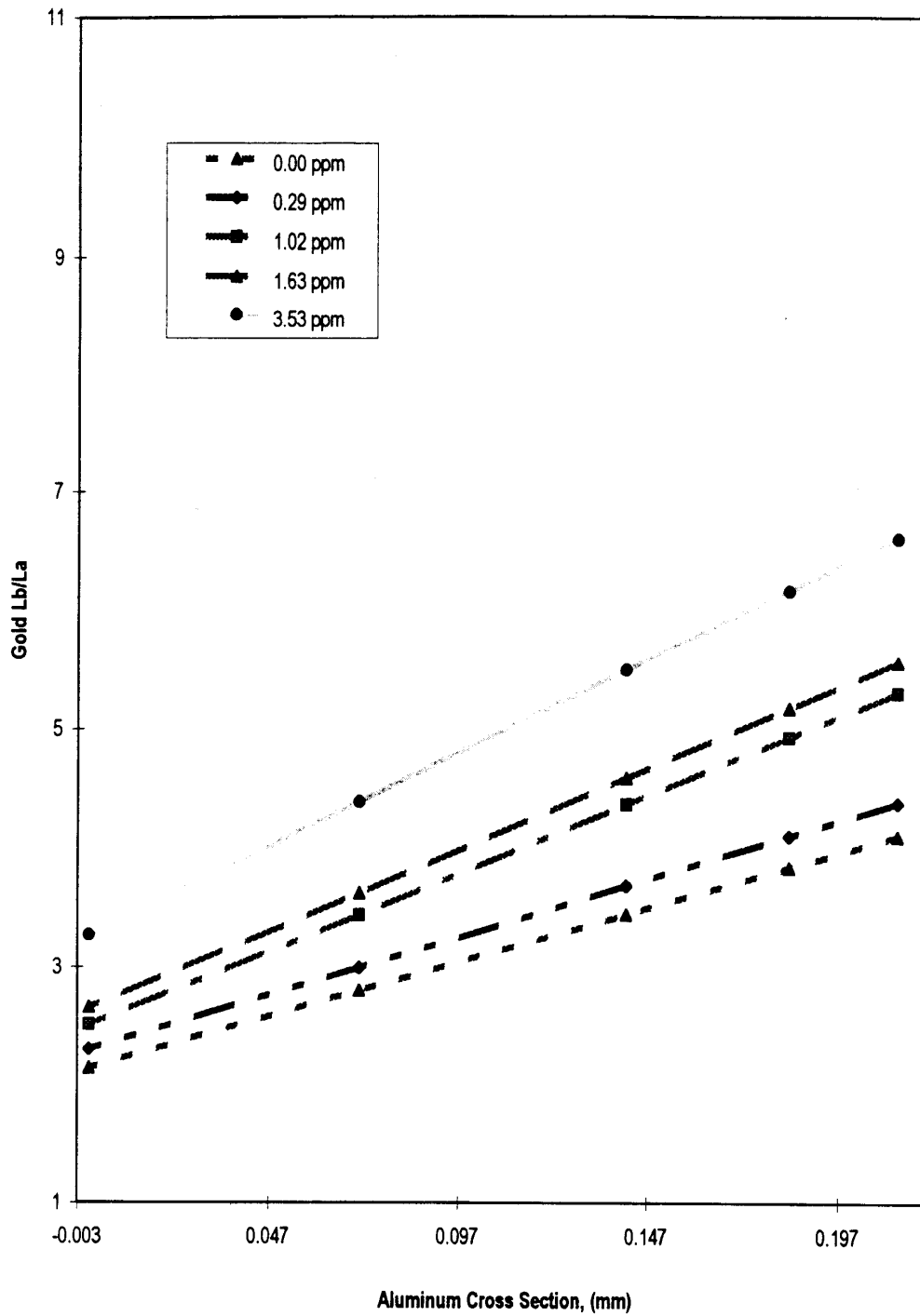


Figure A2: Linear regression lines for varying cross-sections of plastic covers above paint SRM versus the gold L-line ratio.

